

A 3'-Untranslated Region Variant Is Associated With Impaired Expression of CD226 in T and Natural Killer T Cells and Is Associated With Susceptibility to Systemic Lupus Erythematosus

Sara E. Löfgren,¹ Angelica M. Delgado-Vega,¹ Caroline J. Gallant,¹ Elena Sánchez,² Johan Frostegård,³ Lennart Truedsson,⁴ Enrique de Ramón Garrido,⁵ José M. Sabio,⁶ María F. González-Escribano,⁷ Bernardo A. Pons-Estel,⁸ Sandra D'Alfonso,⁹ Torsten Witte,¹⁰ Bernard R. Lauwerys,¹¹ Eموke Endreffy,¹² László Kovács,¹³ Carlos Vasconcelos,¹⁴ Berta Martins da Silva,¹⁵ Javier Martín,² Marta E. Alarcón-Riquelme,¹⁶ and Sergey V. Kozyrev¹

Objective. Costimulatory receptor CD226 plays an important role in T cell activation, differentiation, and cytotoxicity. This study was undertaken to investigate the genetic association of CD226 with susceptibility to systemic lupus erythematosus (SLE) and to assess the functional implications of this association.

Methods. Twelve tag single-nucleotide polymorphisms (SNPs) in CD226 were typed in 1,163 SLE patients and 1,482 healthy control subjects from Europe

or of European ancestry. Analyses of association were performed by single-marker Cochran-Mantel-Haenszel meta-analysis, followed by haplotype analysis. Gene expression was analyzed by quantitative real-time polymerase chain reaction analyses of RNA from peripheral blood mononuclear cells, and by fluorescence-activated cell sorter analysis. To study the functional impact of the associated variants, luciferase reporter constructs containing different portions of the 3'-untranslated

Supported in part by grants from the Wenner-Gren Foundation (to Dr. Gallant); from FISM, Regione Piemonte (CIPE and Ricerca Sanitaria Finalizzata grant 2008 to Dr. D'Alfonso); from the BMBF Kompetenznetz Rheuma C2.12, Germany (to Dr. Witte); from the Spanish Ministry of Science and the Andalusian Science Department (grants SAF2006-00398 and CTS-1180 to Dr. Martín); from the European Commission (CVDIMMUNE project grant LSHM-CT-2006-037227), the Swedish Research Council for Medicine, the Swedish Association Against Rheumatism, the Magnus Bergwalls Foundation, the King Gustaf V's 80-Year Foundation, the Torsten and Ragnar Söderbergs Foundation, and the Marcus Borsgröms Foundation (to Dr. Alarcón-Riquelme); and from the Swedish Rheumatism Association, the Clas Groschinskys Foundation, and the King Gustaf V's 80-Year Foundation (to Dr. Kozyrev). Dr. Pons-Estel's work was supported in part by a research grant from the Federico Wihelm Agrícola Foundation; he also is the coordinator of the Argentine Collaborative Group.

¹Sara E. Löfgren, MSc, Angelica M. Delgado-Vega, MD, Caroline J. Gallant, PhD, Sergey V. Kozyrev, PhD: Uppsala University, Uppsala, Sweden; ²Elena Sánchez, PhD, Javier Martín, MD, PhD: CSIC, Granada, Spain; ³Johan Frostegård, MD, PhD: Karolinska University Hospital, Huddinge, Stockholm, Sweden; ⁴Lennart Truedsson, MD, PhD: Lund University, Lund, Sweden; ⁵Enrique de Ramón Garrido, MD, PhD: Hospital Carlos Haya, Málaga, Spain; ⁶José M. Sabio, MD, PhD: Hospital Virgen de las Nieves, Granada, Spain; ⁷María F. González-Escribano, PhD: Hospital Virgen del Rocío, Seville, Spain; ⁸Bernardo A. Pons-Estel, MD: Sanatorio Parque, Rosario, Argentina; ⁹Sandra D'Alfonso, PhD: University of Eastern

Piedmont, Novara, Italy; ¹⁰Torsten Witte, MD, PhD: Hannover Medical School, Hannover, Germany; ¹¹Bernard R. Lauwerys, MD, PhD: Cliniques Universitaires Saint-Luc and Université Catholique de Louvain, Brussels, Belgium; ¹²Eموke Endreffy, PhD: University of Szeged, Szeged, Hungary; ¹³László Kovács, MD, PhD: Albert Szent-Györgyi Clinical Centre and University of Szeged, Szeged, Hungary; ¹⁴Carlos Vasconcelos, MD, PhD: Hospital Santo Antonio and Instituto de Ciências Biomédicas Abel Salazar, Porto, Portugal; ¹⁵Berta Martins da Silva, PhD: Instituto de Ciências Biomédicas Abel Salazar and Universidade do Porto, Porto, Portugal; ¹⁶Marta E. Alarcón-Riquelme, MD, PhD: Uppsala University, Uppsala, Sweden, CSIC, Granada, Spain, Oklahoma Medical Research Foundation, Oklahoma City, and Center for Genomics and Oncological Research, Pfizer—University of Granada—Junta de Andalucía, Granada, Spain.

Ms Löfgren and Dr. Delgado-Vega contributed equally to this work. Drs. Alarcón-Riquelme and Kozyrev contributed equally to this work.

Dr. Kovács has received consulting fees, speaking fees, and/or honoraria from Abbott, UCB, and Schering-Plough (less than \$10,000 each). Dr. Vasconcelos has received consulting fees, speaking fees, and/or honoraria from Roche, Pfizer, Janssen-Cilag, Gilead Sciences, and Merck, Sharp, and Dohme (less than \$10,000 each).

Address correspondence and reprint requests to Sergey V. Kozyrev, PhD: Department of Genetics and Pathology, Rudbeck Laboratory, Uppsala University, Dag Hammarskjölds väg 20, 751 85 Uppsala, Sweden. E-mail: sergey.kozyrev@genpat.uu.se.

Submitted for publication March 12, 2010; accepted in revised form July 20, 2010.

region (3'-UTR) of the gene were prepared and used in transfection experiments.

Results. A 3-variant haplotype, rs763361; rs34794968;rs727088 (ATC), in the last exon of *CD226* was associated with SLE ($P = 1.3 \times 10^{-4}$, odds ratio 1.24, 95% confidence interval 1.11–1.38). This risk haplotype correlated with low *CD226* transcript expression and low *CD226* protein levels on the surface of CD4+ and CD8+ T cells and natural killer T (NKT) cells. NK cells expressed high levels of *CD226*, but this expression was independent of the haplotype. Reporter assays with deletion constructs indicated that only the presence of rs727088 could account for the differences in the levels of luciferase transcripts.

Conclusion. This study identified an association of *CD226* with SLE in individuals of European ancestry. These data support the importance of the 3'-UTR SNP rs727088 in the regulation of *CD226* transcription both in T cells and in NKT cells.

Systemic lupus erythematosus (SLE) is a prototypical autoimmune disease with a wide range of clinical manifestations. It is characterized by the production of autoantibodies against nuclear antigens and increased apoptosis of leukocytes, together with impaired mechanisms of clearance, which leads to the formation and deposition of immune complexes in multiple organs. The disease has a complex inheritance, with a number of genes contributing to susceptibility to SLE. In addition, some of the implicated genes are shared with other autoimmune diseases, which suggests that there are common pathogenic pathways (1).

A recent genome-wide association study in patients with type 1 diabetes identified a susceptibility, nonsynonymous risk variant in *CD226* (rs763361/Gly³⁰⁷Ser) (2), located on chromosome 18q22.3 (3). The association of rs763361 has been further observed recently in studies of patients with multiple sclerosis, autoimmune thyroid disease, rheumatoid arthritis, and Wegener's granulomatosis (4,5). However, whether *CD226* is a susceptibility gene for SLE is not yet known. Interestingly, *CD226* levels on the surface of T cells are altered in SLE patients (6). Moreover, *CD226* expression is specifically down-regulated in natural killer T cells (NKT cells) in patients with active SLE, which, in turn, is correlated with increased sensitivity of these cells to anti-CD95-induced apoptosis (7).

CD226, a type I transmembrane receptor of the immunoglobulin superfamily that has 2 immunoglobulin-like extracellular domains, is predominantly expressed on the surface of T cells and NK cells and is

also present on monocytes, platelets, a subset of B cells (3), mast cells (8), and megakaryocytes (9). *CD226* is involved in the activation and differentiation of T cells (10–12), adhesion and cytotoxicity of T cells and NK cells (3,13), apoptosis (7,14), transendothelial migration of monocytes (15), and activation and aggregation of platelets (16,17).

CD226 recognizes, with similar binding affinity, 2 ligands present on the target cells: nectin-2/CD112 and poliovirus receptor/CD155 (18,13). Engagement with the ligands induces phosphorylation of the cytoplasmic domain by protein kinase C (19) and by the Src family kinase Fyn (20), which provides a costimulatory signal for activation of T and NK cells (11).

In the present study, we identify, for the first time, an association of *CD226* with SLE in patients of European ancestry through a risk haplotype located in the 3'-untranslated region (3'-UTR). In addition, we demonstrate that the risk allele C of rs727088 is responsible for the reduced gene expression of *CD226* in T and NKT cells.

PATIENTS AND METHODS

Patients and controls. After quality control of the data, the cohort consisted of 1,163 patients with SLE and 1,482 ethnicity-matched healthy control subjects from the European multicenter collaboration (see Appendix for the collaborative group participants) known as the BIOLUPUS network (supported by the European Science Foundation), comprising individuals from Argentina (60 patients and 109 controls), Belgium (70 patients and 59 controls), Germany (284 patients and 176 controls), Hungary (38 patients and 35 controls), Italy (264 patients and 320 controls), Portugal (163 patients and 165 controls), Spain (206 patients and 227 controls), and Sweden (78 patients and 391 controls). All of the individuals from Argentina had >85% European ancestry. Patients who did not fulfill at least 4 of the American College of Rheumatology 1982 criteria for the classification of SLE (21) were excluded from the study. In addition, subjects with an individual genotyping rate lower than 90%, as well as duplicated and/or related samples, were excluded. Non-European individuals ($n = 61$), who were identified by principal components analysis, were also removed from the study cohort.

Single-nucleotide polymorphism (SNP) selection. From the linkage disequilibrium (LD) structure of the *CD226* locus in the HapMap CEU population (data release 27; available at <http://hapmap.ncbi.nlm.nih.gov/>), 12 tag SNPs capturing the variation at the gene locus including 20 kb upstream and downstream of the gene, with a minor allele frequency of greater than or equal to 10% and an r^2 threshold of greater than or equal to 0.8, were selected using the tagger algorithm implemented in Haploview, version 4.1 (22). The rs763361 SNP was forced-included in the list of SNPs.

Genotyping. All samples were genotyped at the Feinstein Institute for Medical Research (Manhasset, NY) using a

GoldenGate Custom Genotyping Assay and a BeadXpress Reader from Illumina. Three SNPs (rs727088, rs34794968, and rs763361) were genotyped by TaqMan 5'-exonuclease assay (Applied Biosystems) at Uppsala University and at the Instituto de Biomedicina y Parasitología López-Neyra in Granada (for all samples from Spanish subjects). Genotyping consistency between the centers has been established as being near 100% (23).

Genetic association analysis. The genetic association analysis was done using PLINK software, version 1.07 (24). First, all SNPs with a genotype call rate lower than 95% or those not in Hardy-Weinberg equilibrium ($P < 0.001$) were excluded. For the single-marker tests, we performed a Cochran-Mantel-Haenszel (CMH) meta-analysis, using the country of origin as the stratification variable, and also performed a Breslow-Day test to assess the homogeneity of the odds ratios (ORs). In addition, we performed a haplotype analysis of the 3'-UTR block, including a general, or omnibus, test, a sliding window analysis with 2 SNPs and 3 SNPs, and haplotype-specific association tests implemented in PLINK (24). The omnibus haplotype test is a global test of association in which the alternate hypothesis of each haplotype having a unique effect is compared with the null hypothesis of no haplotypes having any different effect (24). The haplotype-specific analysis involves testing of each haplotype against all others pooled together (1 df) (24), and interpretation of the ORs derived from this test must take into account the fact that there is no single reference haplotype in the analysis. Alternative genetic models (additive, dominant, and recessive) for the haplotype association were tested by logistic regression using R, version 2.9.2.

For analyses of RNA expression and fluorescence-activated cell sorter (FACS) analyses, statistical calculations were performed using an unpaired 2-tailed *t*-test with GraphPad software (available at <http://www.graphpad.com>). The correlation between relative expression levels of RNA and genotypes was analyzed by linear regression using PLINK software, version 1.07. The original expression data were normalized using an exponential transformation (log normal distribution).

Transcript analysis and gene resequencing. We performed analysis of all gene transcripts expressed in the subjects' peripheral blood mononuclear cells (PBMCs) and in samples of human thymus (Clontech). Primers specific to different areas of the coding region were as follows: for forward primers, forward transcript CD226, GCGTTAGAGC-GAGCAGCACTCACATCTC, forward exon 2, TCAAA-CAGTTTCCAGAGATGGATTA, and forward cd226, CGT-GATGAGATTGACTGTAGCCGA; for reverse primers, reverse transcript CD226, GCTTAATCTCCCCTGGATCAT-TCTG, reverse cd226, GGGTGCCTTCTGTGTATCCCAG, and reverse exon 3, AGGGAAGTGTATGCCAAAGC. Commercial common adapter primers Ap1 and Ap2 were used for polymerase chain reaction (PCR) analysis of human thymus complementary DNA (cDNA). The GenBank accession number for the novel alternative Δexon2–3 transcript is GU935336. Approximately 500 bp of the promoter region, exon 1, exons 2 and 3, exons 5 and 7, and ~500 bp of the adjacent introns, as well as the region downstream of the gene, were sequenced in samples from 35 individuals of Swedish origin.

Analysis of CD226 messenger RNA (mRNA) expression. Total RNA was purified with TRIzol reagent (Invitrogen) from PBMCs obtained from 84 healthy donors of Swedish origin. Synthesis of cDNA was performed at 42°C for 80 minutes using 2 μg of RNA, 5 μM oligo(dT) primer, Moloney murine leukemia virus transcriptase, and RNase inhibitor in buffer supplemented with 5 mM MgCl₂ and 1 mM dNTP. The TRIzol interphase left after RNA purification was used for purification of genomic DNA for further genotyping and cloning.

CD226 expression was determined by quantitative real-time PCR on a 7900HT Sequence Detection System (Applied Biosystems) with version 2.2.2 software, using SYBR Green for signal detection. The following primer pairs were used: forward CGTGATGAGATTGACTGTAGCCGA, and reverse GGGTGCCTTCTGTGTATCCCAG. Initial denaturation at 95°C for 5 minutes was followed by 45 cycles comprising 95°C for 15 seconds, 66°C for 15 seconds, and 72°C for 15 seconds. The PCR buffer was supplemented with 1.5 mM MgCl₂, 200 μM dNTP, primers, SYBR Green (Molecular Probes), 15 ng of cDNA, and 0.5 units of Platinum Taq polymerase (Invitrogen). Expression levels were normalized to the gene coding for TATA-binding protein (TBP) using the comparative 2^{-ΔC_t} method (25). Real-time PCR for TBP was performed with commercial reagents (Applied Biosystems). All experiments were run in triplicate.

Cell preparation and FACS analysis of CD226 surface expression. Freshly collected buffy coats, obtained at the Uppsala University Hospital from 100 healthy donors, were aliquoted and immediately frozen in liquid nitrogen with 10% DMSO (Sigma). An aliquot was used for DNA purification and subsequent genotyping. Frozen cells that had been obtained from individuals with known genotypes (total of 22 individuals; 8 women and 14 men) were thawed, and leukocytes were purified from erythrocytes by lysing in ACK lysing buffer (Gibco) for 4 minutes, followed by centrifugation at 500g for 5 minutes, washing in phosphate buffered saline (PBS) buffer, and staining with antibodies for FACS analysis.

Three-color flow cytometry was used for quantitative measurement of CD226 in total lymphocytes, CD3+CD4+ T cells, CD3+CD8+ T cells, CD3–CD19+ B cells, CD3–CD56+ NK cells, and CD3+CD56+ NKT cells. Purified leukocytes were resuspended in PBS and incubated with different combinations of antibodies: phycoerythrin (PE)–Cy5–conjugated CD3 (clone HIT3a), fluorescein isothiocyanate (FITC)–conjugated CD4 (RPA-T4), FITC–conjugated CD8 (RPA-T8), Alexa Fluor 488–conjugated CD56 (B159), allophycocyanin-Cy7–conjugated CD19 (HIB19), and PE–conjugated CD226 (DX11) for 30 minutes at room temperature. Background fluorescence was assessed using appropriate isotype- and fluorochrome-matched control antibodies. All antibodies were purchased from BD Biosciences, except for HIB19, which was obtained from BioLegend. Twenty thousand lymphocytes were acquired on an LSR II FACS using DiVA software (BD Biosciences), and data analysis was performed using FlowJo software (TreeStar).

Reporter constructs and luciferase assays. The entire exon 7 coding for the 3'-UTR region and ~500 bp of the downstream sequence of the human CD226 gene was amplified by PCR analysis of samples from individuals with known genotypes. The following primers were used: forward GCAC-

Table 1. Association analysis of *CD226* single-nucleotide polymorphisms (SNPs) with systemic lupus erythematosus*

SNP	Basepair position†	Location	Allele A	Allele A frequency	Allele B	OR	95% CI	P_{CMH}	$P_{CMH-corrected}$	$P_{Breslow-Day}$	Genotyping rate, %	P_{HWE} vs. controls
rs12604328	65675953	Downstream	C	0.29	T	1.18	1.04–1.33	0.0100	0.0299	0.1202	99.74	0.8455
rs1469858	65680197	Downstream	T	0.43	C	1.15	1.03–1.29	0.0144	0.0344	0.2197	99.89	0.5563
rs727088	65681419	Exon 7	C	0.50	T	1.21	1.08–1.36	9.57×10^{-4}	0.0105	0.1812	97.88	0.3711
rs34794968	65682006	Exon 7	T	0.42	G	1.17	1.04–1.31	8.51×10^{-3}	0.0299	0.1320	98.79	0.7454
rs763361	65682622	Exon 7	A	0.50	G	1.20	1.07–1.35	1.74×10^{-3}	0.0105	0.1366	98.83	0.2499
rs1124980	65699607	Intron 4	C	0.43	T	1.15	1.02–1.29	0.0180	0.0359	0.5640	99.92	0.8304
rs12969613	65710412	Intron 4	T	0.49	A	1.13	1.01–1.27	0.0331	0.0496	0.1627	99.92	0.4351
rs17208329	65716443	Intron 3	T	0.23	C	1.10	0.96–1.26	0.1732	0.2079	0.2659	99.85	0.7099
rs17842596	65716559	Intron 3	C	0.42	T	1.11	0.99–1.25	0.0745	0.0993	0.1146	99.81	0.5899
rs1788234	65717567	Intron 3	T	0.40	C	1.14	1.02–1.28	0.0255	0.0438	0.1662	99.47	0.0912
rs10432228	65719229	Intron 3	C	0.32	T	1.00	0.89–1.13	0.9424	0.9424	0.4305	99.96	0.1894
rs11151547	65751971	Intron 3	C	0.47	T	1.06	0.94–1.19	0.3400	0.3709	0.8565	99.85	0.2496

* The odds ratios (ORs) (with 95% confidence intervals [95% CIs]) were calculated for the frequency of allele A in each SNP, determined using a Cochran-Mantel-Haenszel meta-analysis with the country of origin as the stratification variable. The value P_{CMH} indicates the significance of the allelic association determined by the Cochran-Mantel-Haenszel meta-analysis, while $P_{CMH-corrected}$ displays the association after adjustment for false discovery rate, and $P_{Breslow-Day}$ is the P value determined using the Breslow-Day test for homogeneity of the ORs. P_{HWE} is the P value testing for Hardy-Weinberg equilibrium in patients compared with healthy controls. The analyses were performed using PLINK software, version 1.07 (24).

† Obtained from the National Center for Biotechnology Information Build 36.

CCAATAACTATAGAAAGTCCCATC, and reverse TATACCTGGATTCATGAAATGT. *Pfu* Ultra II Fusion HS DNA polymerase was used with *Pfu* Ultra II buffer (Stratagene) supplemented with 200 μ M dNTP (Invitrogen), primers, and 15 ng of genomic DNA. Initial denaturation at 95°C for 5 minutes was followed by 30 cycles comprising 95°C for 15 seconds, 60°C for 15 seconds, and 72°C for 2 minutes. The PCR products were purified from gel and were then cloned in the pGL3-promoter vector (Promega) by replacing the vector's original SV40 late poly(A) sequence. The constructs with the full-length 3'-UTR and 3 more deletion constructs for each allele were prepared and verified by sequencing.

Subsequently, 800 ng of the luciferase reporter constructs were cotransfected together with 10 ng pRL-TK vector (Promega) in 3×10^5 HEK 293 T cells using Lipofectamine 2000 (Invitrogen). Thirty hours after transfection, cells were collected, washed with PBS, and then lysed in Passive Lysis Buffer (Promega). Ten microliters of the protein lysates was assayed with a dual-luciferase reporter assay system (Promega). Values for luciferase activity were normalized, with results expressed as the ratio of *Firefly* to *Renilla* luciferase units. Independent plasmid purifications, transfections, and luciferase assays were repeated 4 times.

Assessment of RNA degradation rates. The kinetics of mRNA degradation were measured after treatment of the cells with actinomycin D. Briefly, 30 hours after transfection with the reporter constructs, cells were treated with 10 μ g/ml of actinomycin D (Sigma) and collected at 0, 2, 4, 8, and 12 hours thereafter. RNA and DNA were purified using TRIzol and then processed for quantitative real-time PCR. In order to control for transfection efficiency, transcript levels were normalized to the levels of plasmid DNA assessed by quantitative PCR. The following primers matching to the luciferase gene were used for both RNA and DNA PCRs: forward CATTCTATCCGCTGGAAGATGGAAC, and reverse TCATAGCTTCTGCCAACCGAACG.

RESULTS

Association of *CD226* with susceptibility to SLE.

To examine the role of *CD226* in SLE, we first performed a search for new common variants in the gene by sequencing 500 bp from the proximal promoter, exon 1, exons 2 and 3, exons 5 and 7, ~500 bp of the intronic sequence surrounding each exon, and 500 bp downstream of the gene in 35 individuals. Two insertion/deletions were identified. Deletion GGGGGCT, located downstream of exon 1, was present in all of the samples, and insertion/deletion AGTG, located 223 bp downstream of the gene, displayed a pattern correlating with SNP rs727088, the closest variant located in the 3'-UTR of *CD226*. The C allele of rs727088 correlated with the presence of the insertion, while the T allele correlated with the deletion. No other polymorphisms in the sequenced regions were found.

We next genotyped 12 tag SNPs, including rs763361, and tested for associations in 1,163 SLE patients and 1,482 ethnicity-matched healthy controls (Table 1). Association analyses revealed that the strongest significant signal was in exon 7 of *CD226* (for rs763361, corrected P value in the CMH meta-analysis [$P_{CMH-corrected}$] = 0.0105, OR 1.20, 95% confidence interval [95% CI] 1.07–1.35); for rs34794968, $P_{CMH-corrected}$ = 0.0299, OR 1.17, 95% CI 1.04–1.31; and for rs727088, $P_{CMH-corrected}$ = 0.0105, OR 1.21, 95% CI 1.08–1.36). These 3 SNPs were strongly correlated and were part of a 5-SNP haplotype block covering the last exon and 5 kb downstream of the gene

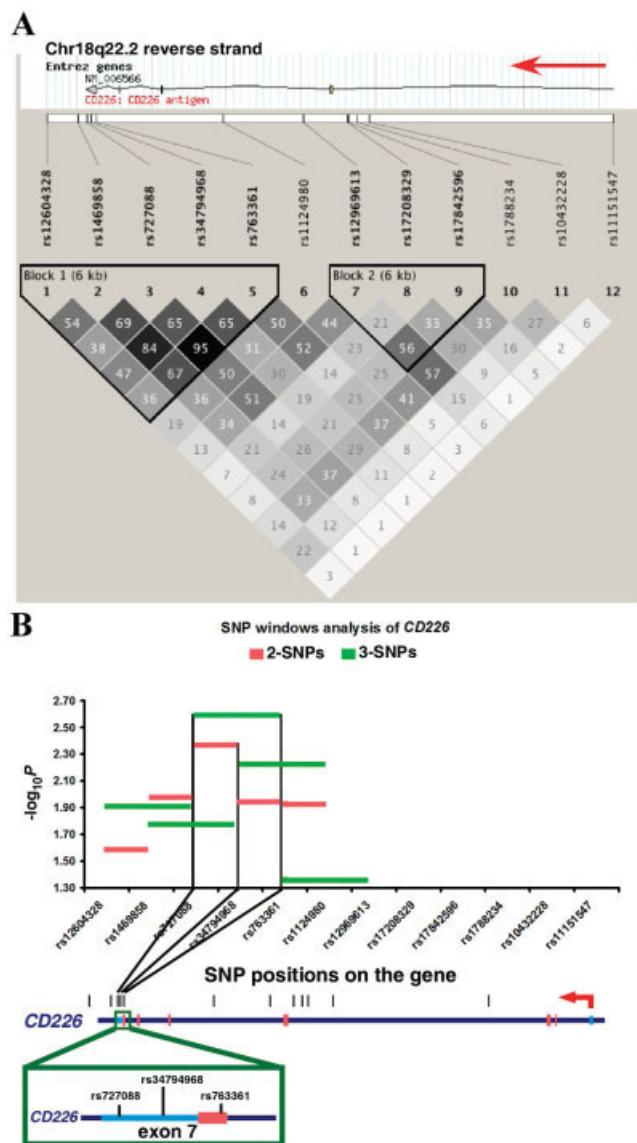


(Figure 1A). The 5-SNP haplotype block was associated with disease status ($P = 0.0163$, by omnibus test).

Table 2. Association of the *CD226* haplotype block rs763361–rs727088 in exon 7

	Frequency			OR (95% CI)
	Cases	Controls	P	
Global*			5.26×10^{-4}	
Haplotype-specific†				
GGT	0.479	0.511	0.100	0.91 (0.82–1.02)
ATC	0.443	0.397	1.30×10^{-4}	1.24 (1.11–1.38)
AGC	0.078	0.091	0.122	0.868 (0.70–1.00)

* The global P value indicates the overall significance of the association of the rs763361;rs34794968;rs727088 haplotype, determined using the omnibus haplotype test of association.

† In haplotype-specific analyses, the odds ratio (OR) with 95% confidence interval (95% CI) was determined for each allele variant in haplotype rs763361;rs34794968;rs727088 tested against all of the others pooled together. For this test, there is no single reference haplotype, and the OR must be interpreted in this context. All analyses were performed using PLINK software, version 1.07 (24).

The high correlation between the alleles of these SNPs made it difficult to discern the true susceptibility variant, and therefore, in an attempt to dissect the association of this block, we performed several haplotype tests. First, we examined whether any SNP had an effect independent of the haplotype background. However, this was not possible to test, due to the high LD between the SNPs, which thus meant the absence of common haplotypes (those with a frequency of >0.05) containing all of the possible allele combinations. We then tested for association using a sliding window of 2 and 3 SNPs, which narrowed down the association region to the 3'-UTR in between SNPs rs34794968 and rs727088, since both were included in the 2 best windows (Figure 1B). The best model of association was observed in the haplotype combination rs763361;rs34794968;rs727088 ($P = 8.63 \times 10^{-4}$, by omnibus test). These variants formed 3 common haplotypes: GGT, ATC, and AGC (Table 2). By testing each haplotype against all others, only one, ATC, was found to be consistently associated with SLE ($P = 1.30 \times 10^{-4}$, OR 1.24, 95% CI 1.11–1.38).

We also tested alternative genetic models. The association of the haplotype ATC fitted an additive model best ($P = 0.000123$). However, the recessive model showed the strongest impact in terms of the effect size ($P = 0.0011$, OR 1.40 95% CI 1.14–1.71).

***CD226* mRNA expression in leukocytes.** In order to determine whether the associated 3'-UTR haplotype correlated with gene expression, we measured *CD226* mRNA expression levels in the PBMCs of healthy donors. We first performed analysis of all gene transcripts expressed in PBMCs and samples of human thymus. Two alternative transcripts were detected in the

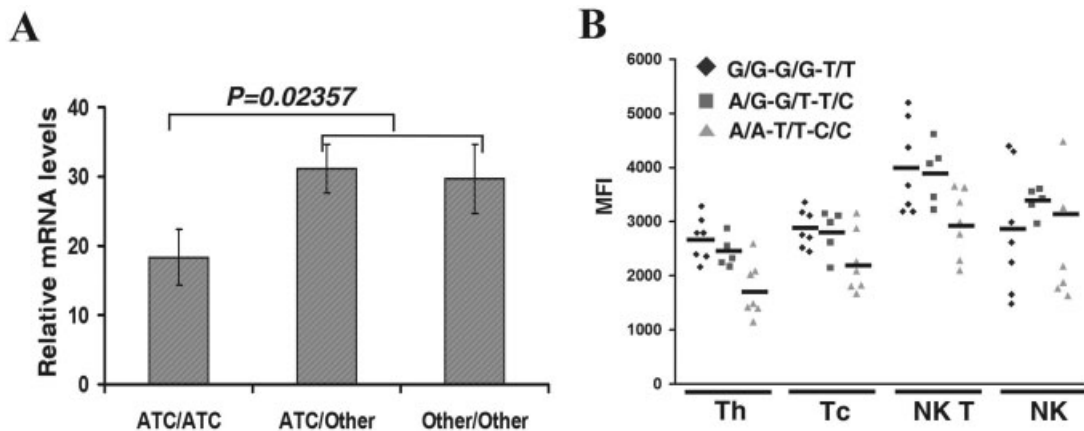


Figure 2. Differential expression of *CD226*. **A**, For analysis of *CD226* mRNA expression in peripheral blood mononuclear cells from healthy donors, samples were stratified according to haplotypes made up of rs763361, rs34794968, and rs727088. A recessive genetic effect is shown by the significant difference in mRNA expression between the ATC/ATC homozygotes and those with the ATC/Other or Other/Other haplotypes (includes GGT and the less-frequent AGC). Bars show the mean \pm SD relative mRNA levels normalized to the housekeeping gene coding for the TATA-binding protein. **B**, Surface expression of *CD226* protein was analyzed by fluorescence-activated cell sorter analysis in T helper (CD4+) cells (Th), T cytotoxic (CD8+) cells (Tc), natural killer T (CD3+CD56+) cells (NKT), and natural killer (CD3-CD56+) cells (NK) from individuals grouped according to A/A-T/T-C/C homozygotes ($n = 7$), A/G-G/T-T/C heterozygotes ($n = 5$), and G/G-G/G-T/T homozygotes ($n = 7$). Bars show the mean. Differences in mean values between the ATC and GGT groups were as follows: $P = 0.0022$ for Th cells, $P = 0.0295$ for Tc cells, $P = 0.0264$ for NKT cells, and $P = 0.7092$ for NK cells. MFI = mean fluorescence intensity.

PBMCs: the full-length isoform, and the Δ exon2-3 isoform (lacking exons 2 and 3). The presence of the Δ exon2-3 transcript, which, because of exon-skipping, contains a shift in the translational-reading frame, may lead to the premature termination of protein synthesis. We evaluated the relative amounts of the transcripts and found that Δ exon2-3 transcripts were present at very low levels when compared with those of the full-length isoform (results not shown).

We next analyzed the expression of the full-length isoform of *CD226* in the PBMCs of healthy individuals, in whom different 3'-UTR haplotypes were present. In total, the analysis included 13 individuals who were homozygous for the haplotype ATC (ATC/ATC), 38 in whom only 1 copy of the ATC haplotype plus any other haplotype was present (ATC/other), and 33 in whom either GGT or the low-frequency AGC haplotype, but no copies of the ATC haplotype, was present (other/other). We found that individuals homozygous for the risk haplotype ATC expressed the lowest *CD226* transcript levels ($P = 0.02357$) compared with the heterozygous group or those homozygous for other haplotypes (Figure 2A). This result suggests that there is a recessive effect of the ATC haplotype on gene expression levels. We also tested these associations in the additive and dominant models, but neither yielded

significant results ($P = 0.083$ and $P = 0.415$, respectively).

Surface expression of *CD226* protein. For measurement of *CD226* protein expression on the surface of different populations of lymphocytes from individuals with different haplotypes, we used FACS analysis. The highest levels of surface expression of *CD226* were observed on NKT cells, cytotoxic T cells, and NK cells. We observed that individuals with the haplotype ATC had significantly lower surface expression of *CD226* than did individuals with the GGT haplotype, specifically in T helper cells (CD3+CD4+) ($P = 0.0022$), T cytotoxic cells (CD3+CD8+) ($P = 0.0295$), and NKT cells (CD3+CD56+) ($P = 0.0264$) (Figure 2B). None of the individuals had the low-frequency haplotype AGC in the cell analysis. Both the mean values for *CD226* surface expression and the lack of statistically significant differences in expression between the GGT haplotype and the heterozygote haplotypes further confirmed the significance of the recessive model observed in the RNA expression analysis.

The number of cells staining positive for *CD226* was similar among individuals with different genotypes, indicating that the correlation of the down-regulation of *CD226* expression with the risk haplotype was not attributable to reduced cell numbers in any of the

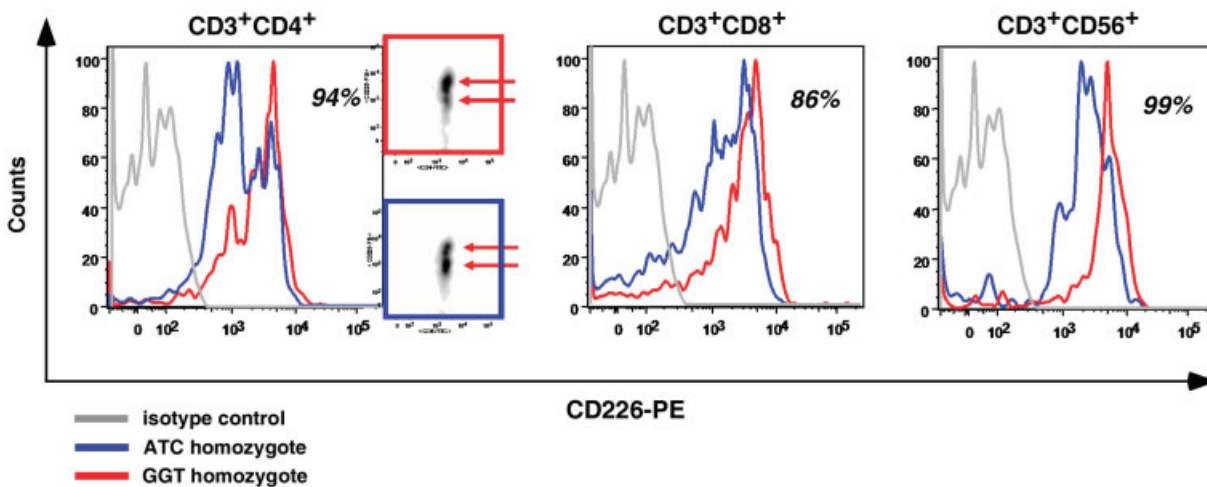


Figure 3. Fluorescence-activated cell sorter (FACS) analysis of CD226 surface staining. FACS histograms show the log mean fluorescence intensity values (determined by staining with phycoerythrin-conjugated CD226 antibodies [CD226-PE]) plotted against the cell counts for the cell subpopulations CD3+CD4+, CD3+CD8+, and CD3+CD56+ in individuals with either the ATC haplotype or GGT haplotype, compared with isotype control. Results are from 1 representative individual of 7 in each genotype group, and percentages of positive cells are shown as averages. The gray-scale density plots on the right side of the CD3+CD4+ histogram show the relative frequencies of subpopulations of CD4+ cells expressing CD226. The red arrows indicate the 2 varying subpopulations observed in the individuals with the ATC or GGT haplotype.

analyzed subpopulations but rather to a transcriptional down-regulation of *CD226*. Interestingly, staining with anti-CD226 antibodies revealed the presence of 2 subpopulations of CD4+ T cells that differentially expressed CD226 (Figure 3). Moreover, CD226 expression in the CD4+ cell subsets correlated with haplotype, in that cells from individuals with the low-risk GGT haplotype displayed a major subset of CD4+ cells producing high levels of CD226 and a small fraction of cells producing lower levels, while the opposite pattern was observed in those with the high-risk ATC haplotype. Although NK cells expressed high amounts of surface CD226, comparable with that in CD8+ cells, we could not detect any difference in expression in this cell population between individuals with the low-risk haplotypes and those with the high-risk haplotype ($P = 0.7092$). Furthermore, no difference in expression was observed in B cells (results not shown).

Minigene analysis of the SNPs in the 3'-UTR.

Our association analysis clearly pointed to the last exon of *CD226* between the SNPs rs763361 and rs727088 as the region with the strongest association with SLE. In order to study the independent functional impact of the polymorphisms on gene expression, we prepared 2 haplotype-specific reporter constructs with firefly luciferase and the entire 3'-UTR sequence from the *CD226* gene, along with the 500-bp region downstream of the

poly(A) site (Figure 4A). We prepared 3 more constructs for each haplotype, which included a sequential deletion of the following regions: 1) deletion of 57 nucleotides from the 5'-end, thus lacking SNP rs763361 ($\Delta 76$), 2) deletion of the upstream region, including SNP rs34794968 ($\Delta 347$), and 3) deletion of the region upstream and downstream of rs727088, including the insertion/deletion (short). Constructs were transfected in HEK 293 T cells, and 30 hours later, the activity of luciferase was measured in the protein lysates.

Analysis of these deletion constructs indicated that rs727088 was still significantly associated with differential expression of the luciferase reporter after all other variants were excluded from the construct ($P = 0.01$). In contrast, removal of rs763361, located at the beginning of exon 7 and previously suggested to function in regulation of transcription (4), had no impact on the difference in the levels of luciferase detected. Thus, the evidence suggests that only rs727088, located 245 bp upstream of the poly(A) signal, accounts for the difference in the levels of luciferase transcripts.

Analysis of RNA degradation rate. To investigate the effect of the polymorphisms on RNA turnover, we performed an RNA degradation experiment using 2 haplotype-specific constructs: $\Delta 76$ -T, containing the G allele of rs34794968, the T allele of rs727088, and the deletion, and $\Delta 76$ -C, containing the T allele of

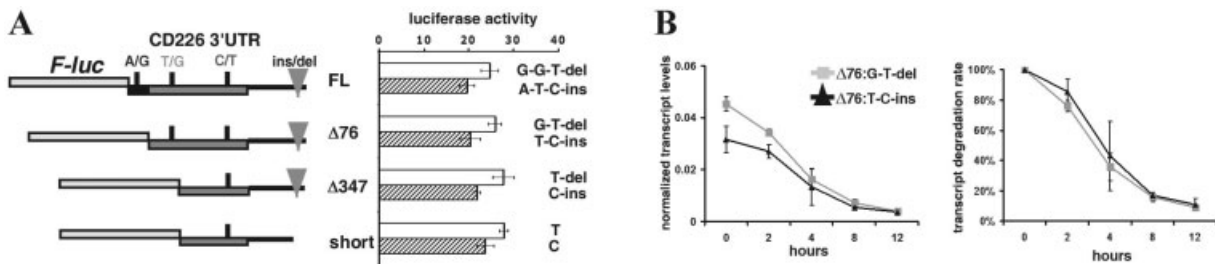


Figure 4. Reporter analysis of the 3'-untranslated region (3'-UTR) of *CD226*. **A**, The entire exon 7 and 500 bp of the downstream region were cloned and inserted after the *firefly* luciferase (*F-luc*) cDNA in a pGL3 vector. **Left**, Deletion (Δ) constructs of each of the variants, except rs727088, are shown with the relative positions for rs763361 (A/G), rs34794968 (T/G), and rs727088 (C/T), along with their respective insertion/deletion (ins/del). **Right**, The relative luciferase activity units of each construct are shown. Bars show the mean \pm SD results from 4 independent experiments. In experiments with the *firefly* luciferase (FL) constructs, $P = 0.02$ for G-G-T-del versus A-T-C-ins; in those with $\Delta 76$, $P = 0.007$ for G-T-del versus T-C-ins; in those with $\Delta 347$, $P = 0.003$ for T-del versus C-ins; and in those with the short constructs, $P = 0.01$ for short T versus short C. **B**, The kinetics of luciferase mRNA degradation in experiments using the 2 reporter constructs, $\Delta 76$ with the alleles G-T-del and $\Delta 76$ with the alleles T-C-ins, were measured after treatment of the cells with actinomycin D. Normalized transcript levels are shown (**left**), as well as transcript levels as a percentage of the initial RNA (**right**). Bars show the mean \pm SD.

rs34794968, the C allele of rs727088, and the insertion. We observed no difference in the luciferase mRNA degradation rates between the experiments with each construct (Figure 4B). Although the initial RNA levels were different, the kinetics of degradation of RNA bearing either the G-T-deletion or the T-C-insertion haplotypes was similar, thus ruling out the possibility that these polymorphisms determined the mRNA degradation rate.

DISCUSSION

Our results provide strong evidence to support the association of SLE with *CD226*, a gene that has been reported to be associated with other autoimmune diseases. We identified a susceptibility haplotype located in the last exon that was formed by 3 highly correlated variants: the rs763361 (Gly³⁰⁷Ser) variant, rs34794968, and rs727088. SNP rs727088 is a novel functional variant that was responsible for reduced gene expression. There are several possible reasons to explain why this variant was not identified before. First, the replication study in patients with type 1 diabetes and those with multiple sclerosis (4), which was based on tag SNPs, did not directly test this variant, most likely because of the complete LD reported in the HapMap CEU population between rs763361 and rs727088. Second, a subsequent association study analyzing an association between *CD266* and Wegener's granulomatosis or multiple sclerosis included only the rs763361 variant (5). Although an association with rs763361 was detected, it cannot be

ruled out that the significant result was due to the high LD with rs727088.

The prior bias toward testing of rs763361 could be attributed mainly to its location as a nonsynonymous variant. Our previous studies on *IRF5* genes (26) and *BANK1* genes (27), as well as the results of the present study, show that a search for other variants, with a focus on the regulatory ones, may lead to more comprehensive understanding of the multiple functional alterations possible within a single gene. We aimed to capture the full genetic variation in the *CD226* 3'-UTR, including several correlated SNPs, so that we could best identify the minimal region of association.

The LD between rs763361 and rs727088 was high in our European cohort ($r^2 = 0.95$) but slightly lower than that in HapMap ($r^2 = 1.00$). The high LD of the region made it difficult to reliably discriminate the true susceptibility variant, due to the lack of haplotypes containing all of the possible allele combinations with a frequency higher than 5%. The inclusion of very rare haplotypes in the analysis introduces a statistical bias, and for that reason, we instead performed functional analyses, which allowed us to separate these alleles in vitro and to better define their functional significance.

Among the tested cell populations, the highest expression of *CD226* was detected on the surface of NKT cells. Moreover, our expression analysis revealed that the risk haplotype ATC, containing the C allele for rs727088, correlated with lower expression of *CD226* in T and NKT cells, but not in NK or B cells. Of note, Tao

et al (7) reported that CD226 was down-regulated specifically on NKT cells of patients with active SLE, suggesting a unique role for these cells in the disease. They found that NKT cells from patients were highly sensitive to apoptosis mediated by the CD95–CD95L or T cell receptor–CD3 pathways. It was demonstrated also that preactivation of CD226 with anti-CD226 antibodies can rescue activated T cells from apoptosis (7).

Reduced numbers and impaired functions of NKT cells were found in both human and mouse lupus (28–33). NKT cells, a subset of regulatory T lymphocytes, are known to control various immune reactions and have been shown to promote immune tolerance (34–38). Recently, Hegde et al (39) have shown that NKT cells may instruct peripheral blood monocytes to develop into myeloid antigen-presenting cells (APCs) with suppressive function and high interleukin-10 production. Furthermore, these APCs silenced T cell responses and inhibited interferon- γ secretion. It has also been observed that NKT cells promote differentiation toward Th2 cells and suppress antibody production in marginal zone B cells in mice (40–42). Thus, the potential role of CD226 in the pathogenesis of autoimmunity might be related to NKT cell-mediated functions. Lower expression of CD226 in susceptible individuals, together with the overall reduction in the NKT cell population, possibly as a result of increased apoptosis, may lead to sustained activation of T cells and thus promote development of autoimmune disorders.

It was previously suggested that the SNP rs763361, located in the beginning of the last exon of CD226, might affect splicing by modifying either exonic splicing enhancers or silencers (2,4). In our study, the removal of the region containing this SNP in the reporter constructs did not reduce the difference in the levels of luciferase, as would be expected if rs763361 were the variant affecting expression. Thus, it is evident that splicing efficiency is unlikely to be the reason for the altered CD226 expression in SLE. An alternative CD226 isoform lacking exon 3 was reported to be present in mice (43). We detected low levels of an isoform lacking exons 2 and 3, which thus generated an untranslated transcript.

However, we cannot exclude the possibility that rs763361 may exert an effect at the protein level by strengthening the adjacent serine–threonine phosphorylation sites Ser³⁰², Ser³⁰⁵, and Thr³⁰⁶ in the cytoplasmic domain of the receptor, as can be predicted using the NetPhosK server program (available at <http://www.cbs.dtu.dk/services/NetPhosK/>), although this needs to be investigated empirically. Nevertheless,

changes in protein phosphorylation could not account for the observed reduction in CD226 transcript levels. Results of the reporter assays indicated that, rather, another SNP, rs727088, is the main variant responsible for the differential gene expression. SNP rs727088 is located 245 bp upstream of the polyadenylation signal and thus may influence the efficiency of transcription termination. We found that RNA turnover was essentially similar for 3'-UTRs with both alleles. At present, the molecular mechanism whereby rs727088 affects the transcription of CD226 needs to be elucidated, especially considering the cell-specific effect of the polymorphism.

In summary, we have identified an association of CD226 with SLE in individuals of European ancestry. Our data support the importance of the 3'-UTR SNP rs727088 for the regulation of CD226 transcription in T and NKT cells.

ACKNOWLEDGMENT

We are grateful to the patients who provided their consent to allow the use of their samples in this and other lupus genetics studies.

AUTHOR CONTRIBUTIONS

All authors were involved in drafting the article or revising it critically for important intellectual content, and all authors approved the final version to be published. Dr. Kozyrev had full access to all of the data in the study and takes responsibility for the integrity of the data and the accuracy of the data analysis.

Study conception and design. Löfgren, Delgado-Vega, Martín, Alarcón-Riquelme, Kozyrev.

Acquisition of data. Löfgren, Delgado-Vega, Sánchez, Frostegård, Truedsson, de Ramón Garrido, Sabio, González-Escribano, Pons-Estel, D'Alfonso, Witte, Lauwerys, Endreffy, Kovács, Vasconcelos, Martins da Silva, Alarcón-Riquelme, Kozyrev.

Analysis and interpretation of data. Löfgren, Delgado-Vega, Gallant, Martín, Alarcón-Riquelme, Kozyrev.

REFERENCES

1. Gregersen PK, Olsson LM. Recent advances in the genetics of autoimmune disease. *Annu Rev Immunol* 2009;27:363–91.
2. Todd JA, Walker NM, Cooper JD, Smyth DJ, Downes K, Plagnol V, et al. Robust associations of four new chromosome regions from genome-wide analyses of type 1 diabetes. *Nat Genet* 2007;39:857–64.
3. Shibuya A, Campbell D, Hannum C, Yssel H, Franz-Bacon K, McClanahan T, et al. DNAM-1, a novel adhesion molecule involved in the cytolytic function of T lymphocytes. *Immunity* 1996;4:573–81.
4. Hafler JP, Maier LM, Cooper JD, Plagnol V, Hinks A, Simmonds MJ, et al. CD226 Gly307Ser association with multiple autoimmune diseases. *Genes Immun* 2009;10:5–10.
5. Wiczorek S, Hoffjan S, Chan A, Rey L, Harper L, Fricke H, et al. Novel association of the CD226 (DNAM-1) Gly307Ser polymorphism in Wegener's granulomatosis and confirmation for multiple sclerosis in German patients. *Genes Immun* 2009;10:591–5.

6. Tabata H, Hara M, Kitani A, Hirose T, Norioka K, Harigai M, et al. Expression of TLI₁SA1 on T cells from patients with rheumatoid arthritis and systemic lupus erythematosus. *Clin Immunol Immunopathol* 1989;52:366–75.
7. Tao D, Shangwu L, Qun W, Yan L, Wei J, Junyan L, et al. CD226 expression deficiency causes high sensitivity to apoptosis in NK T cells from patients with systemic lupus erythematosus. *J Immunol* 2005;174:1281–90.
8. Bachelet I, Munitz A, Mankutad D, Levi-Schaffer F. Mast cell costimulation by CD226/CD112 (DNAM-1/Nectin-2): a novel interface in the allergic process. *J Biol Chem* 2006;281:27190–6.
9. Ma D, Sun Y, Lin D, Wang H, Dai B, Zhang X, et al. CD226 is expressed on the megakaryocytic lineage from hematopoietic stem cells/progenitor cells and involved in its polyploidization. *Eur J Haematol* 2005;74:228–40.
10. Burns GF, Triglia T, Werkmeister JA, Begley CG, Boyd AW. TLI₁SA1, a human T lineage-specific activation antigen involved in the differentiation of cytotoxic T lymphocytes and anomalous killer cells from their precursors. *J Exp Med* 1985;161:1063–78.
11. Shibuya K, Shirakawa J, Kameyama T, Honda S, Tahara-Hanaoka S, Miyamoto A, et al. CD226 (DNAM-1) is involved in lymphocyte function-associated antigen 1 costimulatory signal for naive T cell differentiation and proliferation. *J Exp Med* 2003;198:1829–39.
12. Sherrington PD, Scott JL, Jin B, Simmons D, Dorahy DJ, Lloyd J, et al. TLI₁SA1 (PTA1) activation antigen implicated in T cell differentiation and platelet activation is a member of the immunoglobulin superfamily exhibiting distinctive regulation of expression. *J Biol Chem* 1997;272:21735–44.
13. Tahara-Hanaoka S, Shibuya K, Onoda Y, Zhang H, Yamazaki S, Miyamoto A, et al. Functional characterization of DNAM-1 (CD226) interaction with its ligands PVR (CD155) and nectin-2 (PRR-2/CD112). *Int Immunol* 2004;16:533–8.
14. Fang L, Zhang X, Miao J, Zhao F, Yang K, Zhuang R, et al. Expression of CD226 antagonizes apoptotic cell death in murine thymocytes. *J Immunol* 2009;182:5453–60.
15. Reymond N, Imbert AM, Devillard E, Fabre S, Chabannon C, Xerri L, et al. DNAM-1 and PVR regulate monocyte migration through endothelial junctions. *J Exp Med* 2004;199:1331–41.
16. Scott JL, Dunn SM, Jin B, Hillam AJ, Walton S, Berndt MC, et al. Characterization of a novel membrane glycoprotein involved in platelet activation. *J Biol Chem* 1989;264:13475–82.
17. Kojima H, Kanada H, Shimizu S, Kasama E, Shibuya K, Nakauchi H, et al. CD226 mediates platelet and megakaryocytic cell adhesion to vascular endothelial cells. *J Biol Chem* 2003;278:36748–53.
18. Bottino C, Castriconi R, Pende D, Rivera P, Nanni M, Carnemolla B, et al. Identification of PVR (CD155) and nectin-2 (CD112) as cell surface ligands for the human DNAM-1 (CD226) activating molecule. *J Exp Med* 2003;198:557–67.
19. Shibuya A, Lanier LL, Phillips JH. Protein kinase C is involved in the regulation of both signaling and adhesion mediated by DNAM-1 accessory molecule-1 receptor. *J Immunol* 1998;161:1671–6.
20. Shibuya K, Lanier LL, Phillips JH, Ochs HD, Shimizu K, Nakayama E, et al. Physical and functional association of LFA-1 with DNAM-1 adhesion molecule. *Immunity* 1999;11:615–23.
21. Tan EM, Cohen AS, Fries JF, Masi AT, McShane DJ, Rothfield NF, et al. The 1982 revised criteria for the classification of systemic lupus erythematosus. *Arthritis Rheum* 1982;25:1271–7.
22. Barrett JC, Fry B, Maller J, Daly MJ. Haploview: analysis and visualization of LD and haplotype maps. *Bioinformatics* 2005;21:263–5.
23. Sanchez E, Abelson AK, Sabio JM, Gonzalez-Gay MA, Ortego-Centeno N, Jimenez-Alonso J, et al. Association of a CD24 gene polymorphism with susceptibility to systemic lupus erythematosus. *Arthritis Rheum* 2007;56:3080–6.
24. Purcell S, Daly MJ, Sham PC. WHAP: haplotype-based association analysis. *Bioinformatics* 2007;23:255–6.
25. Livak KJ, Schmittgen TD. Analysis of relative gene expression data using real-time quantitative PCR and the 2^{-ΔC_T} method. *Methods* 2001;25:402–8.
26. Graham RR, Kozyrev SV, Baechler EC, Reddy MV, Plenge RM, Bauer JW, et al. A common haplotype of interferon regulatory factor 5 (IRF5) regulates splicing and expression and is associated with increased risk of systemic lupus erythematosus. *Nat Genet* 2006;38:550–5.
27. Kozyrev SV, Abelson AK, Wojcik J, Zaghlool A, Linga Reddy MV, Sanchez E, et al. Functional variants in the B-cell gene BANK1 are associated with systemic lupus erythematosus. *Nat Genet* 2008;40:211–6.
28. Takeda K, Dennert G. The development of autoimmunity in C57BL/6 lpr mice correlates with the disappearance of natural killer type 1-positive cells: evidence for their suppressive action on bone marrow stem cell proliferation, B cell immunoglobulin secretion, and autoimmune symptoms. *J Exp Med* 1993;177:155–64.
29. Mieza MA, Itoh T, Cui JQ, Makino Y, Kawano T, Tsuchida K, et al. Selective reduction of Vα14+ NK T cells associated with disease development in autoimmune-prone mice. *J Immunol* 1996;156:4035–40.
30. Oishi Y, Sumida T, Sakamoto A, Kita Y, Kurasawa K, Nawata Y, et al. Selective reduction and recovery of invariant Vα24JαQ T cell receptor T cells in correlation with disease activity in patients with systemic lupus erythematosus. *J Rheumatol* 2001;28:275–83.
31. Van der Vliet HJ, von Blomberg BM, Nishi N, Reijm M, Voskuyl AE, van Bodegraven AA, et al. Circulating Vα24+ Vβ11+ NKT cell numbers are decreased in a wide variety of diseases that are characterized by autoreactive tissue damage. *Clin Immunol* 2001;100:144–8.
32. Kojo S, Adachi Y, Keino H, Taniguchi M, Sumida T. Dysfunction of T cell receptor AV24AJ18+,BV11+ double-negative regulatory natural killer T cells in autoimmune diseases. *Arthritis Rheum* 2001;44:1127–38.
33. Green MR, Kennell AS, Larche MJ, Seifert MH, Isenberg DA, Salaman MR. Natural killer T cells in families of patients with systemic lupus erythematosus: their possible role in regulation of IGG production. *Arthritis Rheum* 2007;56:303–10.
34. Yu KO, Porcelli SA. The diverse functions of CD1d-restricted NKT cells and their potential for immunotherapy. *Immunol Lett* 2005;100:42–55.
35. Hammond KJ, Poulton LD, Palmisano LJ, Silveira PA, Godfrey DI, Baxter AG. α/β-T cell receptor (TCR)⁺CD4⁻CD8⁻ (NKT) thymocytes prevent insulin-dependent diabetes mellitus in nonobese diabetic (NOD)/Lt mice by the influence of interleukin (IL)-4 and/or IL-10. *J Exp Med* 1998;187:1047–56.
36. Falcone M, Facciotti F, Ghidoli N, Monti P, Olivieri S, Zaccagnino L, et al. Up-regulation of CD1d expression restores the immunoregulatory function of NKT cells and prevents autoimmune diabetes in nonobese diabetic mice. *J Immunol* 2004;172:5908–16.
37. Jahng AW, Maricic I, Pedersen B, Burdin N, Naidenko O, Kronenberg M, et al. Activation of natural killer T cells potentiates or prevents experimental autoimmune encephalomyelitis. *J Exp Med* 2001;194:1789–99.
38. Sonoda KH, Exley M, Snapper S, Balk SP, Stein-Streilein J. CD1-reactive natural killer T cells are required for development of systemic tolerance through an immune-privileged site. *J Exp Med* 1999;190:1215–26.
39. Hegde S, Jankowska-Gan E, Roenneburg DA, Torrealba J, Burlingham WJ, Gumperz JE. Human NKT cells promote monocyte differentiation into suppressive myeloid antigen-presenting cells. *J Leukoc Biol* 2009;86:757–68.
40. Singh AK, Wilson MT, Hong S, Olivares-Villagomez D, Du C, Stanic AK, et al. Natural killer T cell activation protects mice against experimental autoimmune encephalomyelitis. *J Exp Med* 2001;194:1801–11.
41. Singh AK, Yang JQ, Parekh VV, Wei J, Wang CR, Joyce S, et al.

- The natural killer T cell ligand α -galactosylceramide prevents or promotes pristane-induced lupus in mice. *Eur J Immunol* 2005;35:1143–54.
42. Miellot A, Zhu R, Diem S, Boissier MC, Herbelin A, Bessis N. Activation of invariant NK T cells protects against experimental rheumatoid arthritis by an IL-10-dependent pathway. *Eur J Immunol* 2005;35:3704–13.
 43. Seth S, Georgoudaki AM, Chambers BJ, Qiu Q, Kremmer E, Maier MK, et al. Heterogeneous expression of the adhesion receptor CD226 on murine NK and T cells and its function in NK-mediated killing of immature dendritic cells. *J Leukoc Biol* 2009;86:91–101.

APPENDIX A: PARTICIPANTS IN THE COLLABORATIVE GROUPS

Participants in the Spanish Collaborative Group are Norberto Ortego-Centeno and Jose L. Callejas (Hospital Clínico San Cecilio, Granada), Mayte Camps (Hospital Carlos Haya, Malaga), Juan Jiménez-Alonso (Hospital Virgen de las Nieves, Granada), Julio Sánchez-Román and Francisco J. García-Hernandez (Hospital Virgen del Rocío, Seville), and Miguel Angel López-Nevot (Hospital Virgen de las Nieves, Granada). Participants in the Argentine Collaborative Group are Hugo R. Scherbarth, Pilar C. Marino, and Estela L. Motta (Hospital Interzonal General de Agudos “Dr. Oscar Alende,” Mar del Plata), Susana Gamron, Cristina Drenkard, and Emilia Menso (Hospital Nacional de Clínicas, Universidad Nacional de Córdoba, Córdoba), Alberto Allievi and Guillermo A. Tate (Organización Médica

de Investigación, Buenos Aires), Jose L. Presas (Hospital General de Agudos Dr. Juan A. Fernandez, Buenos Aires), Simon A. Palatnik, Marcelo Abdala, and Mariela Bearzotti (Universidad Nacional de Rosario y Hospital Provincial del Centenario, Rosario), Alejandro Alvarellos, Francisco Caeiro, and Ana Bertoli (Hospital Privado, Centro Medico de Córdoba, Córdoba), Sergio Paira and Susana Roverano (Hospital José M. Cullen, Santa Fe), Cesar E. Graf and Estela Bertero (Hospital San Martín, Paraná), Cesar Caprarulo and Griselda Buchanan (Hospital Felipe Heras, Concordia, Entre Ríos), Carolina Guillerón, Sebastian Grimaudo, and Jorge Manni (Instituto de Investigaciones Médicas “Alfredo Lanari,” Buenos Aires), Luis J. Catoggio, Enrique R. Soriano, and Carlos D. Santos (Hospital Italiano de Buenos Aires y Fundación Dr. Pedro M. Catoggio para el Progreso de la Reumatología, Buenos Aires), Cristina Prigione, Fernando A. Ramos, and Sandra M. Navarro (Hospital Provincial de Rosario, Rosario), Guillermo A. Berbotto, Marisa Jorfen, and Elisa J. Romero (Hospital Escuela Eva Perón, Granadero Baigorria, Rosario), Mercedes A. Garcia, Juan C. Marcos, and Ana I. Marcos (Hospital Interzonal General de Agudos General San Martín, La Plata), Carlos E. Perandones and Alicia Eimon (Centro de Educación Médica e Investigaciones Clínicas, Buenos Aires), and Cristina G. Battagliotti (Hospital de Niños Dr. Orlando Alassia, Santa Fe). Participants in the Italian Collaborative Group are Nadia Barizzone (University of Eastern Piedmont, Novara), Maria Giovanna Danieli (Università Politecnica delle Marche, Ancona), Gian Domenico Sebastiani (U.O.C. di Reumatologia Ospedale San Camillo, Rome), Enrica Bozzolo and Maria Grazia Sabbadini (IRCCS San Raffaele Hospital, Milan), Mauro Galeazzi (Siena University, Siena), and Sergio Migliaresi and Giovanni La Montagna (Second University of Naples, Naples).